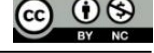




# Düzce University Journal of Science & Technology

Research Article



## Evaluation of the Effect of Land Vegetation on Flood Cross Section in Open Channels

 Esin ACAR <sup>a,\*</sup>

<sup>a</sup> Department of Construction, Borçka Acarlar Vocational School, Artvin Çoruh University, Artvin, TURKEY

\* Corresponding author's e-mail address: esin.acar@artvin.edu.tr

DOI: 10.29130/dubited.1496571

### ABSTRACT

Floods can occur effectively, especially in riverbeds defined as open channels, and can cause damage not only to the riverbed itself but also to the lands located on the right and left banks of the river. In this study, example riverbeds and floodplain areas were utilized. The areas exposed to flooding were planned with different vegetation types and defined by Manning roughness coefficients. By passing a determined flood discharge of  $Q=1000 \text{ m}^3/\text{s}$  through the river cross-section, areas susceptible to flooding were determined using the HEC-RAS program and the standard step method. The influence of vegetation diversity on flooding, the correlation between increasing roughness values and flooding, the acceleration of water velocity by dense vegetation, and the effects of changes in hydraulic radius across sections on flooding were calculated. Additionally, the effects of topographical variations and the selection of roughness coefficients using proper methods on flooding were demonstrated. Thus, the effects of vegetation type, topography, roughness, and hydraulic radius on flood sections were determined and evaluated for their significance.

**Keywords:** Open channels, manning roughness coefficient, flood, land vegetation

## Açık Kanallarda Arazi Vejetasyonunun Taşkın Kesitine Etkisinin Değerlendirilmesi

### Öz

Taşkın, özellikle açık kanal olarak tanımlanan nehir yataklarında etkili bir şekilde oluşabilmektedir ve sadece akarsu yatağını değil aynı zamanda akarsu sağ ve sol sahilinde yer alan araziler için de zarara sebebiyet verebilmektedir. Bu çalışmada örnek olarak oluşturulmuş nehir yatağı ve taşkın alanları kullanılmıştır. Taşkına maruz bırakılan alan farklı vejetasyona sahip olarak planlanarak, manning pürüzlülük katsayıları ile tanımlanmıştır. Belirlenen  $Q=1000 \text{ m}^3/\text{s}$ 'lik taşkın debisi akarsu kesitinden geçirilerek, taşkın hesaplamalarında kullanılan HEC-RAS programı ve standart adım metodu yöntemi ile taşkına maruz kalacak alanlar ortaya konmuştur. Vejetasyon çeşitliliğinin taşkına ne kadar etki ettiği, pürüzlülük değerinin artması ile taşkın arasında bir bağlantının olduğu, su hızını yüksek vejetasyonun arttırdığı, kesitlerdeki hidrolik yarıçapın değişiminin taşkına yapmış olduğu etkiler hesaplanmıştır. Ayrıca topoğrafya farklılıklarından ve doğru metotlarla pürüzlülük katsayılarının seçiminin taşkına etkileri de ortaya konmuştur. Böylece vejetasyon türü, topoğrafya, pürüzlülük ve hidrolik yarıçapın taşkın kesitlerine etkisi belirlenerek, önemi değerlendirilmiştir.

**Anahtar Kelimeler:** Açık kanallar, manning pürüzlülük katsayısı, taşkın, arazi vejetasyonu

## **I. INTRODUCTION**

Floods occurring in open channels, especially in river cross-sections, affect both the living standards and physical conditions of the region. Therefore, the hydraulic evaluation of settlements or vegetation areas within the flood zone will enable taking precautions against potential adverse effects. In this context, hydraulic evaluations of these areas can be carried out using various programs to determine the impacts of flooding. One such program is HEC-RAS, which helps to create floodplains and reveal their hydraulic impacts. Sargin [1] states that flooding is one of the significant disasters to be taken seriously because it involves water overflowing a particular cross-section over time and spreading to surrounding lands, causing economic and social damages. İlhan and Aydar [2] mention that factors affecting the flow of water through the stream (such as debris piles, vegetation, etc.) should be cleaned from the stream to prevent flooding. Onuşluel [3] emphasizes that since floods still cause significant damage in many parts of the world, the relationship between flood characteristics and areas under flood conditions should be thoroughly investigated to cope with flood-induced disasters.

Nowadays, various experimental and numerical modeling studies are used to calculate water surface profiles [4-6]. Knowing the variation of water surface profiles along a channel/river is crucial for the region where that channel/river is located. In hydraulic studies, creating water surface profiles allows for conducting studies using flood cross-sections [7, 8]. According to Yılmaz et al. [9], the HEC-RAS program enables the flood risk analysis of rivers and basins to be conducted in a computer environment, allowing potential problems to be analyzed in advance. Cebe and Bilhan [10] state that the majority of studies using the HEC-RAS model are conducted for flood analysis, while a portion is carried out to simulate water surface profiles.

Çeçen [11] states that during flooding, the variation in vegetation along riverbanks changes the roughness values. The impact of plants along the channel and riverbanks on roughness is significant. The height and type of plants affect roughness. This roughness coefficient is determined using the Manning formula. Water flowing in a river or channel flows at a certain level based on discharge, roughness, and the shape and slope of the open channel.

In this study, a river channel and vegetation were defined on a sample terrain, and with a flood discharge of  $Q=1000 \text{ m}^3/\text{s}$ , the effects of flooding on the river channel and terrain were analyzed using the HEC-RAS program. The study identified the areas submerged according to the specified flood conditions on a specially designed terrain with vegetation and river channel. The unique value of this study lies in providing insights into how to implement flood management practices on lands potentially exposed to flooding by comparing calculations from the example terrain and flood discharge with real-world terrain and computed flood discharge data. In this way, it aims to prevent the negative impacts of floods, especially on agricultural and residential areas. Thus, the impact of vegetation diversity within the sample river channel on flow cross-sections was investigated, and the flood conditions were examined.

## **II. MATERIALS AND METHOD**

In the study, an example riverbed and the land along the riverbanks served as the basis of the work. Different vegetation areas were identified in the riverbed, on the left and right riverbanks, and on the land along the riverbanks. The roughness of these identified vegetation areas was defined using different Manning coefficients. The riverbed was created with a width of 75 meters and a length of 100 meters, and cross-sections were taken every 5 meters for the study. The dimensions specified are entirely based on data from a sample study and have been selected to represent the flood discharge data accurately. This allows the flood-prone areas of the terrain and river channel to be demonstrated on the terrain according to the designated flood discharge. The purpose of this scaling is to create terrain and flood discharge data that can submerge a large portion of the terrain and river channel.

The  $n$  roughness coefficients determined in the study were used in the HEC-RAS program for operational work according to the flood discharges and cross-sections. A flood discharge of  $Q= 1000 \text{ m}^3/\text{s}$  was used, and calculations were made accordingly. The flood discharge data were selected as a discharge level capable of submerging nearly the entire terrain and river cross-section under floodwaters. Özyurt [12] stated that flood events on the Meriç River, which have led to loss of life and property, have prompted plans to protect the Karağaç region from adverse impacts. A drainage channel is planned to safely convey approximately  $1000 \text{ m}^3/\text{s}$  of floodwater downstream along the Meriç River. In this study, additional flood calculations were also performed using the Standard Step Method, which is the operational method of the HEC-RAS program.

The cross-section of the example riverbed and the land along the riverbanks were drawn, and the land vegetation was shown on the plan (Figure 1). This land was created with a wide floodplain and different topography. For the created terrain vegetation, different types of plant cover were estimated. In developing these plant cover types, various vegetation types were considered, including agricultural lands, wooded areas, harvested crops, tree root remnants, and excavated soil areas surrounding the river channel. While calculating the roughness coefficients for these types, composite Manning's  $n$  values were determined based on the roughness values of the terrain at each cross-section. Thus, different Manning's  $n$  roughness values were obtained for the vegetation structure associated with each cross-section. Using these values, varying Manning's  $n$  roughness values were calculated for each section based on the riverbed, right/left slopes, and the different vegetation on the right/left banks of the terrain. Consequently, the velocity values in the flood calculations vary according to different Manning's  $n$  roughness values.

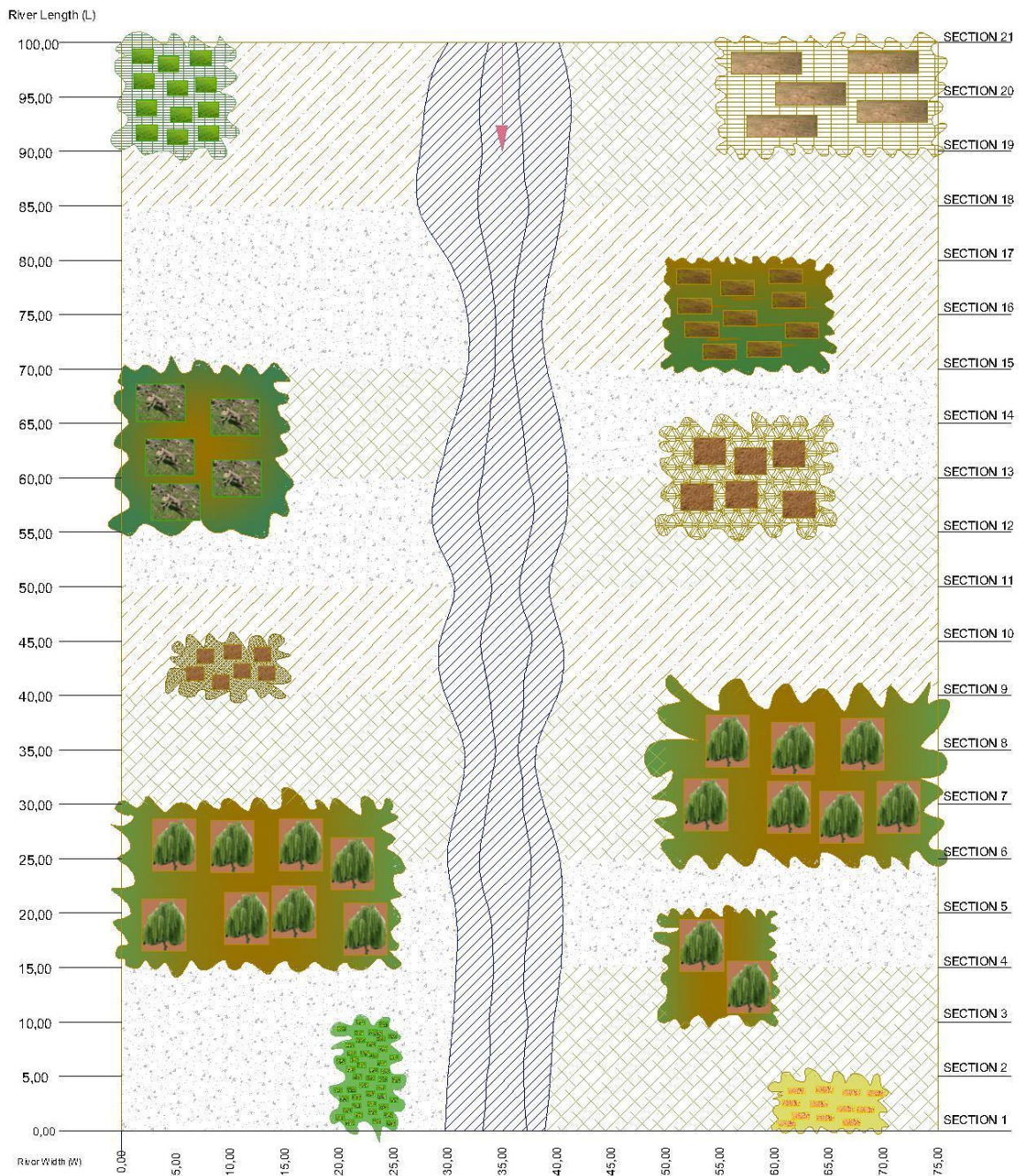


**Figure 1.** Land vegetation

In the study, the Manning-Strickler formula, which is the most commonly used formula in uniform flows, was used (1), where  $V$  represents the average water velocity,  $n$  represents the roughness coefficient,  $R$  represents the hydraulic radius, and  $J$  represents the slope [11]:

$$V = \frac{1}{n} \cdot R^{\frac{2}{3}} \cdot J^{\frac{1}{2}} \tag{1}$$

In this study, the Standard Step Method, which is a method used to determine water surface profiles in river flood calculations, was used. The Froude number calculated in this method is given in Equation

(2). Here,  $V$  represents the average water velocity,  $g$  represents the gravitational acceleration, and  $h$  represents the water depth [13]:

$$F = \frac{V}{\sqrt{gh}} \quad (2)$$

The Standard Step Method can also be applied to non-prismatic channels and, consequently, to natural rivers. In composite (flood section) channels with a second section that has different flow characteristics and even roughness than the main channel, different depths require a different approach for solving the problem [14]. The working principle of the method is shown in Figure 2.

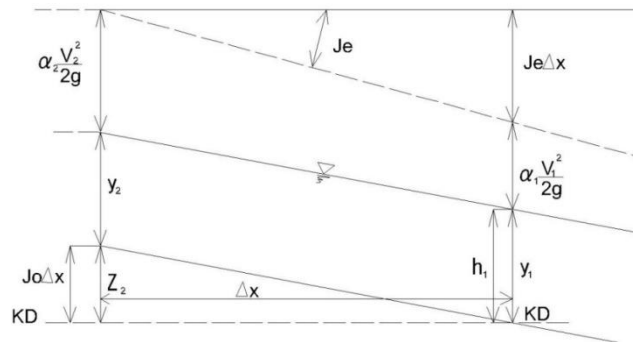


**Figure 2.** Standard Step Method

Water surface calculations are made based on known depths, depending on the nature of the problem. For instance, in river-regime flows, since these flows are controlled by the outlet, the water surface calculation is carried out in the upstream direction, opposite to the flow direction, i.e., from the outlet towards the source. Conversely, in flood-regime flows, the calculation is performed in the downstream direction, from the source towards the outlet [15].

The HEC-RAS program is developed by the Hydrologic Engineering Center (HEC), a division of the Institute of Water Resource (IWR) of the United States Army Corps of Engineers. The program allows for the analysis of one-dimensional steady and unsteady flows, sediment transport analysis, and water temperature analysis [16]. The program is capable of hydraulic modeling in natural rivers, rivers with control structures, cross drainage structures, vertical drop structures, dam breaches, floodgates, culverts, bridges, and other structures [17].

### **A. The effect of land vegetation on flow and Manning roughness coefficient**

In many areas, intensive land use in natural floodplains, such as residential, industrial, or agricultural areas, is quite common. Flood management aims to mitigate or reduce the damage or harm caused by waves through channel scouring and water regulation [18]. Vegetation can either support or suppress turbulent movements and protect riverbanks from erosion [19]. Removing protective vegetation can lead to erosion and flooding [20]. Laws of resistance that define water movement in natural rivers covered with vegetation, known as Manning's roughness coefficients, continue to attract research interest due to their importance for numerous hydrological, ecological, and engineering applications [21].

For the  $n$  Manning roughness values used in the study, friction factors were generally determined using the values presented by Cowan (1956).

In the riverbed cross-section, different roughness values exist at the bed and on the right and left banks. Therefore, calculations were made based on the presence of various roughness values within a section to obtain a single roughness value for the channel [22]. Using the equation below, a single composite roughness value for the main channel has been calculated.

$$n_c = \frac{P_1 n_1 + P_2 n_2 + \dots + P_m n_m}{P} \quad (3)$$

$n_c$ : Composite n roughness value for the channel

$P_1, P_2, P_m$ : Wetted perimeter for the roughness area

$n_1, n_2$ : Roughness coefficient corresponding to the wetted perimeter

$P$ : Total wetted perimeter for the channel

### ***B. River land plan, cross-section, and description of land vegetation***

For use in this study, sample areas have been created on the land, representing riverbeds and areas prone to flooding along the riverbanks. The terrain has been mapped onto the created plan, thus completing the process of mapping the terrain. Based on the terrain, cross-sections and longitudinal sections have been generated. Two different Manning coefficients have been defined for the riverbed, comprising the riverbed itself and the right and left banks. Additionally, different vegetation types present on the land along the riverbanks have been taken into account (Figure 3). Manning roughness ( $n$ ) coefficients, as outlined by Cowan (1956), have been used depending on these vegetation types.

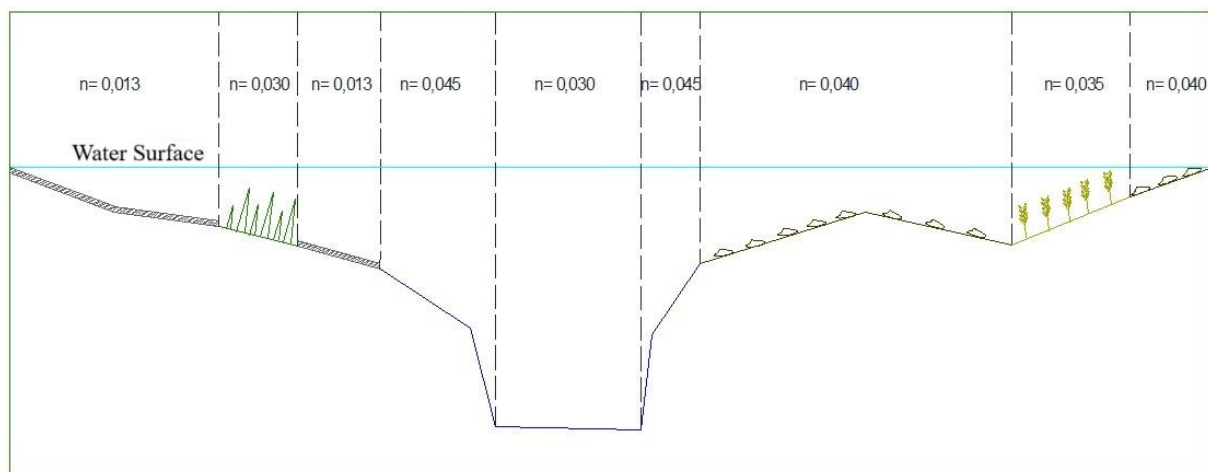


***Figure 3. River type cross section***

Sections have been extracted from the river land plans, and land vegetation and channel roughness have been defined on these sections. The purpose of using different Manning roughness coefficients is to examine the distribution of water on the land during flooding. Thus, different roughness values for each cross-section have altered the water velocity, discharge, and water surface elevations.

### ***C. Hydraulic Evaluations***

The created land is 75 meters wide and 100 meters long, with cross-sections taken every 5 meters for hydraulic calculations. River cross-sections were prepared using the plan of the river land vegetation. Composite (average) roughness values ( $n_c$ ) were calculated using the formulation given in equation (3) in the calculations. Additionally, water depths ( $h$ ) and water surface elevations calculated using the standard step method are provided in Table 1. Furthermore, rigidity ratios were calculated for each cross-section. The rigidity ratio calculation was based on the density of the land vegetation at each cross-section.

**Table 1.** Calculations using the Standard Step Method

Q (m <sup>3</sup> /s)	Section	X (m)	Divided Section	H (m)	A (m <sup>2</sup> )	P (m)	R (m)	R <sup>2</sup> /3	n <sub>c</sub>	K (m <sup>3</sup> /s)	K <sup>3</sup> /A <sup>2</sup>	alfa (velocity coefficient)	V (m/s)	alfa V <sup>2</sup> /2g	H (m)	J <sub>e</sub> = (Q <sup>2</sup> /k <sup>2</sup> )	J <sub>em</sub>	x (m)	h L	H (m)	Fr		
1000	1	0	Main Channel	5,00	30,97	16,07	1,93	1,55	0,041	1,18	0,002												
			Left slope		17,62	38,17	0,46	0,60	0,039	0,27	0,000												
			Right slope		15,95	31,35	0,51	0,64	0,016	0,64	0,001												
			Total		64,54	85,59	0,75	0,83			2,09	0,003	1,28	15,49	15,63	20,6	0,2282		0		20,6	2,2	
	2	5	Main Channel	4,60	30,94	14,95	2,07	1,62	0,041	1,24	0,002												
			Left slope		23,56	37,25	0,63	0,74	0,040	0,43	0,000												
			Right slope		11,17	31	0,36	0,51	0,019	0,30	0,000												
			Total		65,67	83,2	0,79				1,97	0,002	1,32	15,23	15,56	20,2	0,2565	0,2423	5,00	0,47	21,8		
	Main Channel	4,53	30,00	14,3	2,10	1,64	0,041	1,21	0,002														
	Left slope		21,23	37	0,57	0,69	0,040	0,37	0,000														
	Right slope		9,80	29,2	0,34	0,48	0,019	0,25	0,000														
	Total		61,03	80,5	0,76				1,83	0,002	1,37	16,39	18,70	23,2	0,2983	0,2774	5,00	2,60	23,2	2,5			
3	10	Main Channel	4,45	29,80	13,5	2,21	1,70	0,041	1,24	0,002													
		Left slope		25,90	37	0,70	0,79	0,071	0,29	0,000													
		Right slope		9,80	28	0,35	0,50	0,013	0,37	0,001													
		Total		65,50	78,5	0,83				1,90	0,003	1,70	15,27	20,21	24,7	0,2773	0,2878	5,00	1,43	24,7	2,3		
4	15	Main Channel	4,40	26,00	14,00	1,86	1,51	0,037	1,06	0,002													
		Left slope		23,68	35	0,68	0,77	0,036	0,51	0,000													
		Right slope		16,00	31	0,52	0,64	0,102	0,10	0,000													
		Total		65,68	80,00	0,82				1,67	0,002	1,85	15,23	21,86	26,3	0,3580	0,3177	5,00	1,61	26,3	2,3		
5	20	Main Channel	4,15	29,20	13	2,25	1,72	0,038	1,32	0,003													
		Left slope		16,00	25	0,64	0,74	0,013	0,91	0,003													
		Right slope		13,00	21	0,62	0,73	0,125	0,08	0,000													
		Total		58,20	59,00	0,99				2,31	0,006	1,56	17,18	23,48	27,6	0,1866	0,2723	5,00	1,36	27,6	2,7		

Using the standard step method, water surface calculations were performed based on these cross-sections. This method allowed for the creation of water surface profiles for all cross-sections, and water depths (h) and water velocities (V) were calculated (Table 2). A flood discharge of  $Q= 1000 \text{ m}^3/\text{s}$  was used for water surface evaluations.

*Table 2. Section characteristics based on vegetation type in the river channel section*

Section	Channel Length (m)	Section intervals (m)	Channel Base Level (m)	Composite manning ( $n_c$ )	Water Level h (m)	A ( $\text{m}^2$ )	P (m)	R (m)	Water surface elevation	Solid Ratio
1	0	0	245,99	0,04068	5,00	30,97	16,07	1,93	250,99	0,20
2	5	5	248,36	0,04060	4,53	30,00	14,30	2,10	252,89	0,07
3	10	5	250,45	0,04083	4,45	29,80	13,50	2,21	254,90	0,13
4	15	5	251,83	0,03706	4,40	26,00	14,00	1,86	256,23	0,47
5	20	5	253,84	0,03780	4,15	29,20	13,00	2,25	257,99	0,33
6	25	5	254,80	0,03718	4,25	34,60	16,30	2,12	259,05	0,67
7	30	5	255,91	0,03587	4,30	26,00	12,60	2,06	260,21	0,33
8	35	5	256,97	0,03412	4,25	20,12	12,00	1,68	261,22	0,33
9	40	5	258,11	0,06111	3,55	25,00	13,85	1,81	261,66	0,13
10	45	5	259,99	0,05582	3,55	29,00	13,90	2,09	263,54	0,00
11	50	5	261,21	0,05300	3,65	22,00	12,60	1,75	264,86	0,00
12	55	5	262,17	0,05507	3,45	28,00	15,00	1,87	265,62	0,40
13	60	5	264,03	0,05675	3,35	25,00	13,45	1,86	267,38	0,40
14	65	5	266,00	0,05417	3,55	21,13	13,00	1,63	269,55	0,20
15	70	5	267,09	0,09000	3,65	17,84	12,00	1,49	270,74	0,20
16	75	5	269,04	0,08941	3,30	13,00	10,06	1,29	272,34	0,20
17	80	5	272,75	0,08688	3,40	17,00	13,00	1,31	276,15	0,00
18	85	5	273,81	0,04939	2,15	15,10	10,13	1,49	275,96	0,00
19	90	5	274,82	0,04946	2,30	13,93	11,00	1,27	277,12	0,40
20	95	5	275,80	0,04954	2,10	12,74	10,02	1,27	277,90	0,40
21	100	5	275,31	0,04956	2,20	12,74	10,00	1,27	277,51	0,00

The created land topography is shown in Figure 6. Cross-sections and longitudinal sections of the land are drawn based on the land topography.

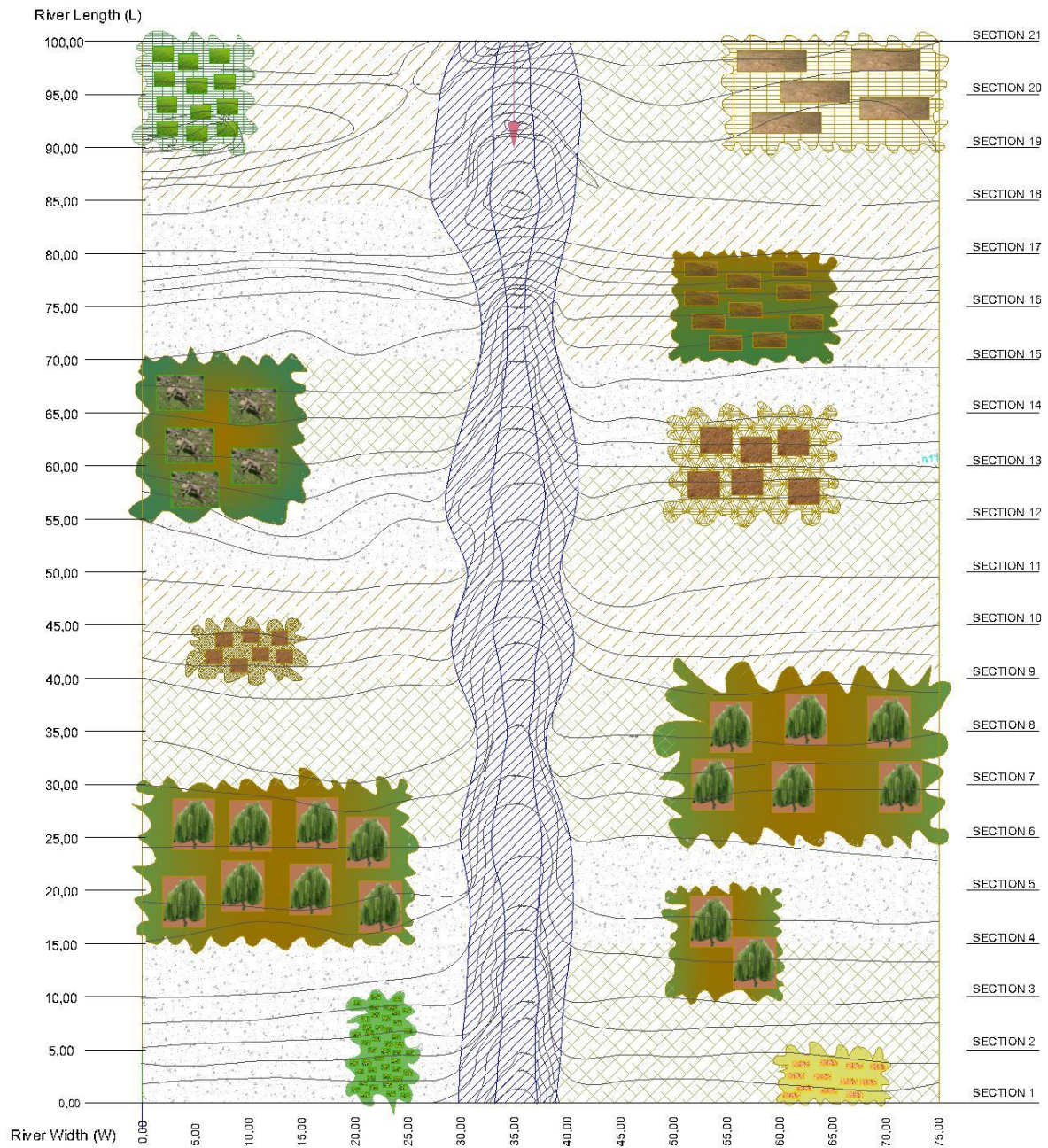


*Figure 4. Land Topography*

The example cross-section extracted from the water surface profiles determined as a result of flood calculations (Figure 5) and the water surface elevations along the land as a longitudinal section processed as an HEC-RAS section (Figure 6) are shown. The water surface profile at the channel bottom is shown in Figure 7.

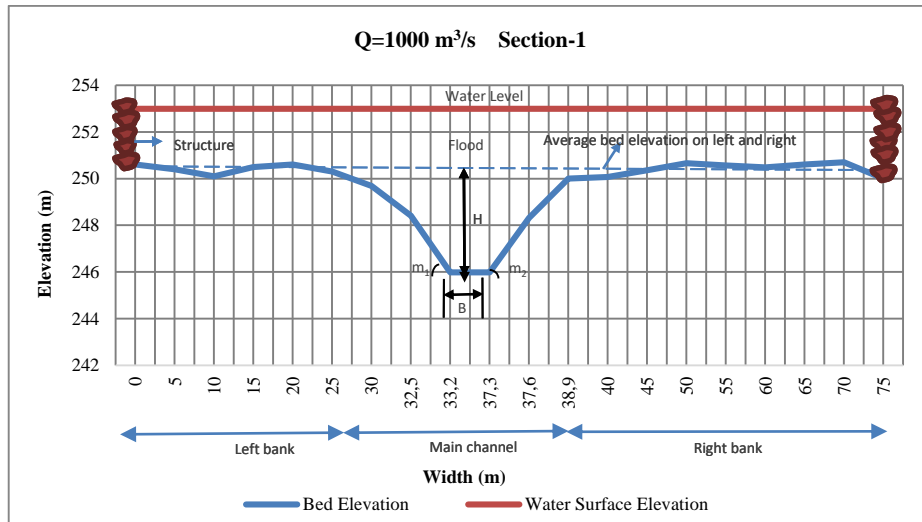


*Figure 5. Channel Cross-section, Section 1*

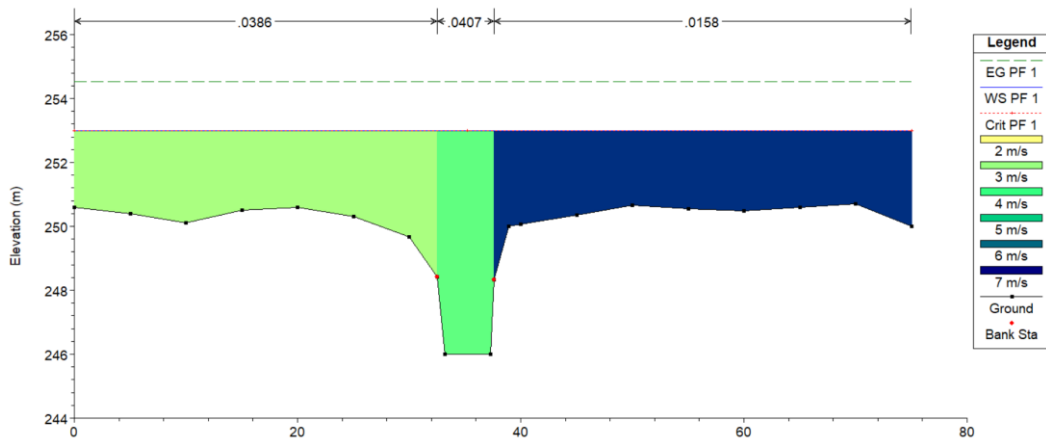


*Figure 6. Channel HEC-RAS Cross-section, Section 1*

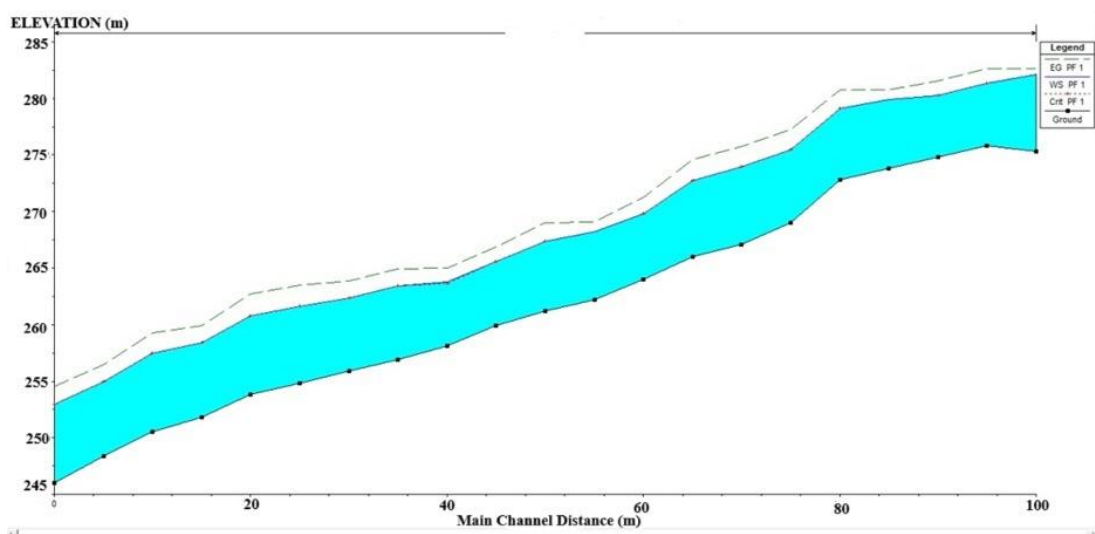


*Figure 7. Water Surface Profile of the Channel*

The map showing the flood area boundaries calculated using the standard step method is shown in Figure 8, the topography of water depth ( $h$ ) is presented in Figure 9, and the velocity ( $V$ ) values are depicted in Figure 10.

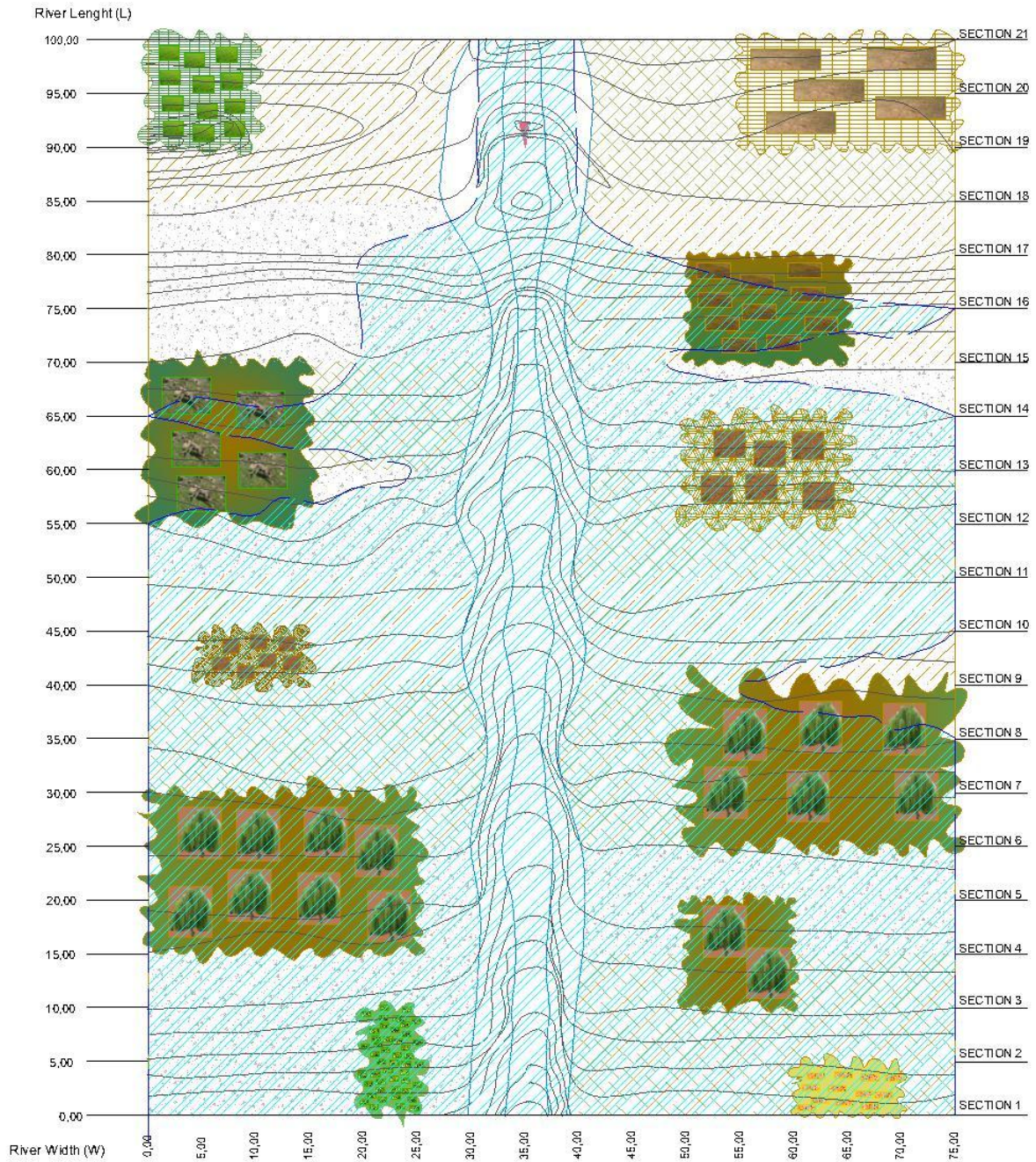


*Figure 8. Flood Area Boundaries*

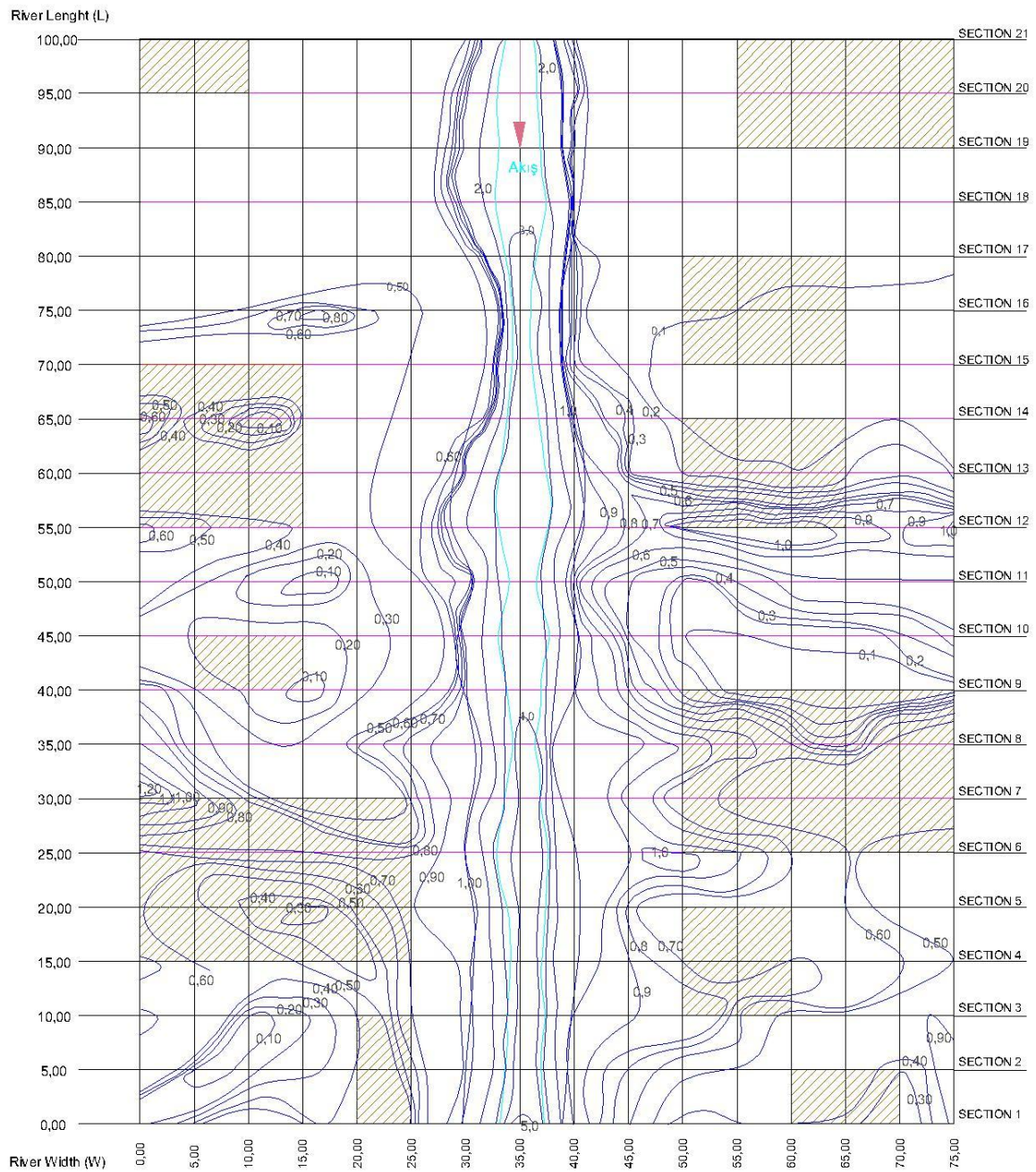


**Figure 9.** Topography of Water Surface Elevations

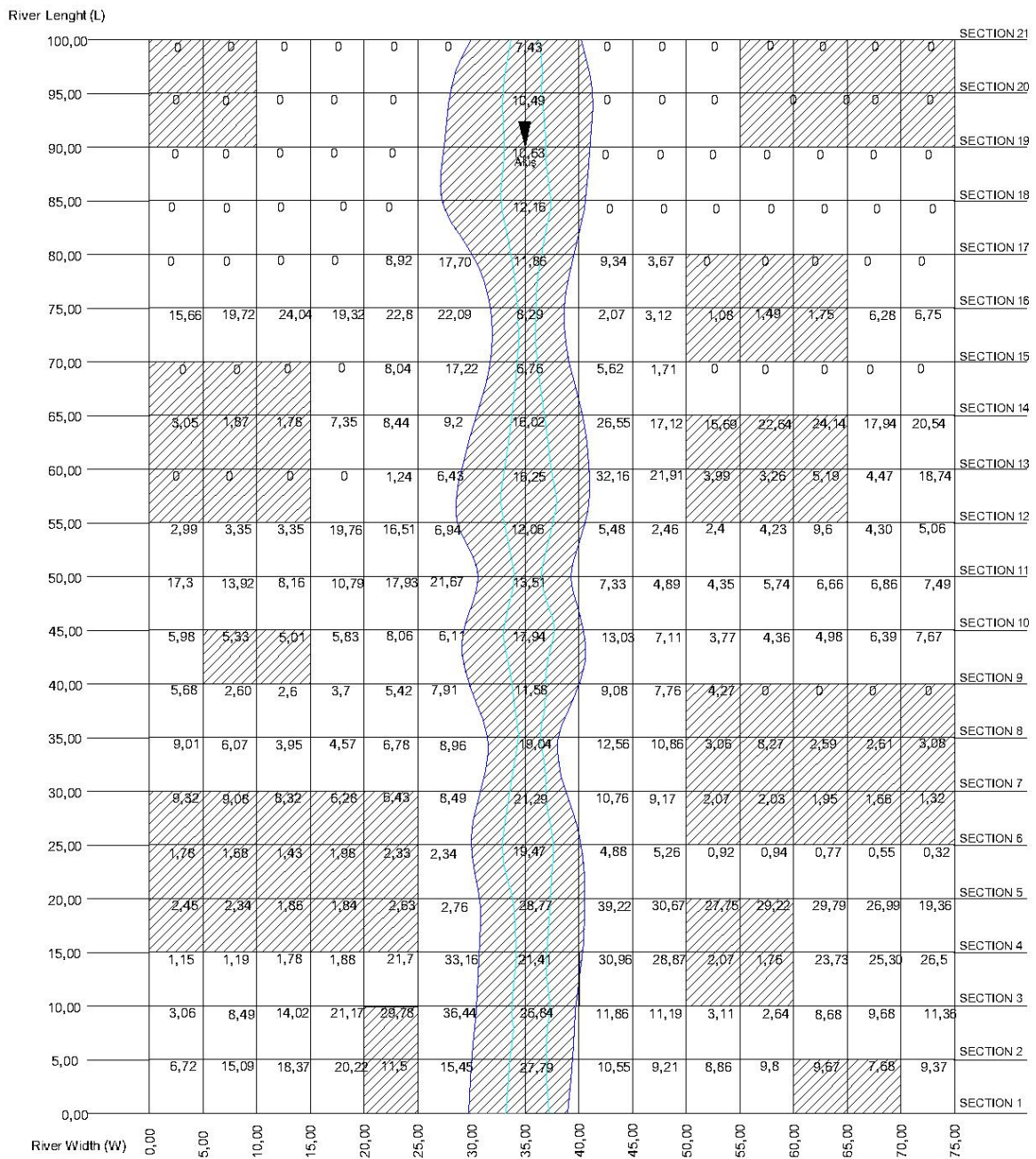


Figure 10. Velocity (V) of Water Flow (m³/s)

## VI. RESULTS

The water surface elevations and velocities calculated using the standard step method based on the determined flood discharge  $Q= 1000 \text{ m}^3/\text{s}$  form the foundation of the study. The impact of vegetation changes on water velocity has been evaluated in the study. Hydraulic calculations were performed using longitudinal sections taken on the land. As an example, Table 3 presents the results obtained from the longitudinal section taken at the 25th meter.",

*Table 3. Hydraulic Calculations for the 25th Meter Longitudinal Section*

Section	Channel Length (m)	Cross-section distance (m)	Level (m)	longitudinal slope (J25)	Manning (n)	h (m)	A (m <sup>2</sup> )	P (m)	R (m)	V (m/s)	Q (m <sup>3</sup> /s)	Fr	Water Surface (m)
1	0	0	250,3	0,0000	0,030	0,45	0,00	0,90	0,00	0,00	0,00	0,00	250,9
2	5	5	252,3	0,4000	0,030	0,48	2,40	5,96	0,40	11,50	27,59	5,30	252,9
3	10	5	254,2	0,3980	0,013	0,59	2,98	6,19	0,48	29,78	88,58	12,3	255,0
4	15	5	255,4	0,2280	0,013	0,55	2,78	6,11	0,45	21,70	60,22	9,30	256,1
5	20	5	257,1	0,3340	0,150	0,73	3,65	6,46	0,57	2,63	9,61	0,98	258,0
6	25	5	258,2	0,2320	0,150	0,82	4,10	6,64	0,62	2,33	9,55	0,82	259,0
7	30	5	259,5	0,2620	0,040	0,41	2,08	5,83	0,36	6,43	13,34	3,19	260,2
8	35	5	260,3	0,1520	0,040	0,75	3,78	6,51	0,58	6,78	25,59	2,49	261,2
9	40	5	261,2	0,1740	0,035	0,35	1,75	5,70	0,31	5,42	9,49	2,93	261,6
10	45	5	263,1	0,3840	0,035	0,35	1,75	5,70	0,31	8,06	14,10	4,35	263,5
11	50	5	264,2	0,2280	0,013	0,39	1,98	5,79	0,34	17,93	35,41	9,11	264,7
12	55	5	265,0	0,1480	0,013	0,50	2,50	6,00	0,42	16,51	41,27	7,45	265,5
13	60	5	267,2	0,4580	0,040	0,02	0,10	5,04	0,02	1,24	0,12	2,80	267,3
14	65	5	269,1	0,3620	0,040	0,50	2,53	6,01	0,42	8,44	21,30	3,79	269,6
15	70	5	270,5	0,2840	0,013	0,09	0,45	5,18	0,09	8,04	3,62	8,56	270,7
16	75	5	271,8	0,2560	0,013	0,55	2,75	6,10	0,45	22,88	62,93	9,85	272,2
17	80	5	276,1	0,8600	0,013	0,04	0,23	5,09	0,04	8,92	2,01	13,4	276,1
18	85	5	276,9	0,1600	0,035	0,00	0,00	0,00	0,00	0,00	0,00		276,9
19	90	5	278,3	0,2980	0,035	0,00	0,00	0,00	0,00	0,00	0,00		278,3
20	95	5	279,1	0,1420	0,035	0,00	0,00	0,00	0,00	0,00	0,00		279,1
21	100	5	278,1	0,2000	0,035	0,00	0,00	0,00	0,00	0,00	0,00		278,1

When Table 3 is evaluated:

When we look at Sections 2 and 3, Section 2 has a Manning roughness coefficient of  $n: 0,030$ ,  $v = 11,50$  m<sup>3</sup>/s, and Section 3 has a Manning roughness coefficient of  $n: 0,013$ ,  $v = 29,78$  m<sup>3</sup>/s. Despite having similar land topography, the difference in velocity values between these two sections is due to the roughness coefficient. A roughness coefficient of  $n: 0,030$  indicates short grass on the land, while  $n: 0,013$  indicates widespread clay soil cover. Consequently, the roughness of the grassy surface significantly reduces the water velocity. On the other hand, the clay soil surface has lower roughness, resulting in accelerated water velocity, reaching nearly three times the previous velocity. When evaluating Sections 4 and 5, the effect of roughness coefficients on velocity ( $V$ ) can be observed. Due to their different roughness, from the clay soil surface in Section 4 to a rough terrain with dense willows in Section 5, the speed drops from 21,7 m/s to 2,63 m/s as the water encounters rough terrain.

However, not only does roughness affect water velocity, but wet area and wet perimeter, i.e., hydraulic radius, also play a role. For example, when examining Sections 13 and 14, although the roughness coefficients are the same at 0,040, the velocities are 1,24 m/s and 8,44 m/s, respectively. This difference is attributed to the wet area and, consequently, the wet perimeter. Section 13 has an area of 0,10 m<sup>2</sup>, while Section 14 has an area of 2,53 m<sup>2</sup>, with similar slopes.

When examining Sections 16 and 17, the velocities are 22,88 m/s and 8,92 m/s, respectively. Although the roughness coefficients are the same at  $n: 0,013$ , the hydraulic radius are 0,45 m and 0,04 m, and the slopes are  $J_{16}:0,2560$  and  $J_{17}: 0,8600$ . Examining the topography between these sections reveals steep terrain. Consequently, the increase in slope leads to an increase in water velocity.

Sudden changes in land topography also affect water velocity and consequently impact flood areas. This is evident in the transition from Section 17 to 16. Additionally, the width of the riverbed also affects water velocity. If there is a riverbed with the same base width, the likelihood of riverbanks being exposed to flooding is lower in a wider riverbed.

The detailed evaluation of the 25th-meter longitudinal section was conducted because it generally represents the hydraulic similarity of the terrain. Therefore, each of the other longitudinal sections was not individually evaluated.

## **IV. CONCLUSION**

In the study, a flood map was created for a sample river channel and terrain cross-section. Within this context, areas exposed to flooding in the river channel and on the terrain based on the designated flood discharge are shown in Figure 8. According to this flood mapping, it was observed that a significant portion of the terrain is submerged. In Figure 9, the water heights ( $h$ ) depicted on the topographic map indicate that water levels are higher in areas near the river cross-section, while lower water levels are observed in more open areas of the terrain. It was particularly noted that the water heights ( $h$ ) are higher in areas affected by existing vegetation on the terrain. In the water velocity ( $V$ ) map shown in Figure 10, it is seen that water velocities are lower in areas with vegetation and that the increase in roughness values decreases water velocity. The results of these mapping studies demonstrate compatibility with the Manning equation.

In the study, the following conclusions were reached regarding the effect of roughness conditions on flood situations in the created riverbed and terrain:

- It was observed that vegetation with high roughness significantly reduces water velocity in flood-prone river basins.

- In riverbed rehabilitation efforts, conducting section-based surveys can reduce flood risks in areas with similar conveyance capacities. This is attributed to the similarity in wetted areas, wetted perimeters, and hence hydraulic radii. Additionally, if the roughness values within the channel are similar, sudden changes in water velocity can be prevented, thereby reducing flood risk.
- It was observed that terrain topography significantly affects water velocity. Particularly, the steep terrain from Section 17 to 16 increases water velocity, leading to higher susceptibility to flooding in that area.

In the study, a flood map was created for a river channel and terrain cross-section generated as an example. Within this scope, areas exposed to flooding in the river channel and on the terrain, based on the determined flood discharge, are shown in Figure 8. According to this flood mapping, it was observed that a large portion of the terrain is submerged. In Figure 9, the water elevations (h) on the topographic map indicate that water levels are higher in areas near the river cross-section and lower in the more open areas of the terrain. It was also noted that water elevations (h) are higher in areas affected by existing vegetation on the terrain. In the water velocity map (V) shown in Figure 10, water velocities are lower in vegetated areas, and the increase in roughness values results in a decrease in water velocity. These mapping study results indicate compatibility with the Manning equation.

The selection of the roughness coefficient is crucial, especially when modeling flood channels. The correct choice of the roughness coefficient will affect the velocity and the water level in the sections, thus influencing the flood situation [23]. Therefore, it is clearly evident from the calculations that high roughness values in flood channels reduce velocity and increase the wetted area, leading to flooding in the region as the water level rises. Another important aspect is the effect of hydraulic radius. The change in wetted area and wetted perimeter will alter the hydraulic radius, so both criteria should be considered in the calculations. Flood management is defined as all efforts made to control floods, identify the triggers of floods, and minimize the effects of floods [24-26]. Particularly in areas with settlements located in streambeds, significant risks can arise. Therefore, especially in planning residential areas, agricultural lands, and other living areas, it is essential to create flood risk assessment maps, which serve as preventive measures against potential disasters.

## Article Information

**Acknowledgments:** The author would like to express their sincere thanks to the editor and the anonymous reviewers for their helpful comments and suggestions.

**Author's Contributions:** Writing—original draft, review, analysis and editing, E.A. Authors have read and approved the final version of it.

**Artificial Intelligence Statement:** No any Artificial Intelligence tool is used in this paper.

**Conflict of Interest Disclosure:** No potential conflict of interest was declared by authors.

**Plagiarism Statement:** This article was scanned by the plagiarism program.

## **V. REFERENCES**

- [1] A. Sargın, “Coğrafi bilgi sistemleri ile taşkın riski ön değerlendirmesi,” T.C. Orman ve Su İşleri Bakanlığı, Technical Report, pp. 1-67, Ankara, 2013.
- [2] S. İlhan and U. Aydar, “İHA görüntülerinden yararlanarak taşkın analizinin yapılması: Çan (Kocabaş) çayı örneği,” *Türkiye İnsansız Hava Araçları Dergisi*, vol. 5, no. 1, pp. 27-36, 2023.
- [3] G. Onuşluel, “Floodplain management based on the HEC-RAS modeling system,” Ph.D. dissertation, Graduate School of Natural and Applied Sciences, Dokuz Eylül University, İzmir, 2005.
- [4] A. M. A. Shaymaa, A. T. A. Sanaa and M. Saad, “Water surface profile and flow pattern simulation over bridge deck slab,” *Journal of Engineering Science and Technology*, vol. 15, no. 1, pp. 291-304, 2020.
- [5] Y. W. Jeong and W. Jeong, “Experimental and numerical investigation of water-surface characteristics at crossing connected non-orthogonally to four flat channels,” *Journal Hydrology and Hydromechanic*, vol. 69, no. 2, pp. 232-242, 2021.
- [6] K. S. Erduran, U. Ünal, A.Ş. Dokuz and M.Ç. Nas, “Köprü ayak tipi ve verevliğinin su yüzü profilleri üzerindeki etkisinin deneysel ve sayısal olarak araştırılması,” *Konjes*, vol. 11, no. 1, pp. 41-58, 2023.
- [7] B. Naik and K. K. Khatua, “Water surface profile computation in nonprismatic compound channels,” *Aquatic Procedia*, vol. 4, pp. 1500-1507, 2015.
- [8] K. S. Erduran, U. Ünal, A. Ş. Dokuz and B. Nas, “Kutu ve dairesel kesitli menfez akımlarının deneysel ve sayısal olarak incelenmesi,” *Niğde Ömer Halisdemir Üniversitesi Mühendislik Bilimleri Dergisi*, vol. 11, no. 4, pp. 1053-1062, 2022.
- [9] N. Yılmaz, H. Bozkurt and Y. Bayazıt, “Akarsu köprülerinin HEC-RAS programı ile hidrolik analizi: fidanlık köprüsü örneği,” *Bilecik Şeyh Edebali Üniversitesi Fen Bilimleri Dergisi*, vol. 7, no. 2, pp. 896-910, 2020.
- [10] K. Cebe, K and Ö. Bilhan, “HEC-RAS hidrodinamik model kullanılarak kararlı akım analizi: Nevşehir, Türkiye örneği,” *Avrupa Bilim ve Teknoloji Dergisi*, vol. 32, pp. 135-141, 2021.
- [11] K. Çeçen, *Hidrolik Cilt II, Açık Kanallar*, İstanbul, Türkiye: İstanbul Teknik Üniversitesi İnşaat Fakültesi Matbaası, 1982.
- [12] N. N. Özyurt, (2020). Su yapıları, 9. hafta, taşkın kontrolü, [PowerPoint slides]. [Online]. Available: [https://yunus.hacettepe.edu.tr/~nozyurt/SuYapilari\\_9.pdf](https://yunus.hacettepe.edu.tr/~nozyurt/SuYapilari_9.pdf).
- [13] N. Orhan, “Derin kuyu pompalarında kritik dalma derinliğinin boyutsuz büyüklükler ile ilişkisi,” *Gazi Üniversitesi Mühendislik Mimarlık Fakültesi Dergisi*, vol. 39, no. 1, pp. 177-190, 2023.
- [14] Y. Yüksel, *Akışkanlar Mekaniği ve Hidrolik*, İstanbul, Türkiye: Beta Basım Yayım, 2020.
- [15] T. Özbek, *Açık Kanal Akımlarının Hidroliği ve Hidrolik Yapılar*, Ankara, Türkiye: Teknik Yayınevi, 2009.
- [16] İ. Tuncer, “Açık kanallarda su yüzü profilinin belirlenmesi, Nakkaş Dere örneğinde bir Hec-Ras uygulaması,” Yüksek Lisans Tezi, Fen Bilimleri Enstitüsü, Gazi Üniversitesi, Ankara, 2011.

- [17] Y. Tektaş and N. Polat, "HEC-RAS ile taşkın modelleme ve Sentinel-2 uzaktan algılama görüntüsünden taşkın hasar analizi: Diyarbakır ili Çakmak Deresi Çınar bölgesi örneği", *Tuzal*, vol. 3, no. 1, pp. 28–35, 2021.
- [18] [18] T. Helmiö and J. Järvelä, "Hydraulic aspects of environmental flood management in boreal conditions," *Boreal Environment Research*, vol. 9, pp. 227-241, 2004.
- [19] A. Murota, T. Fukuhara and M. Sato, "Turbulence structure in vegetated open channel flows," *Journal of Hydrologic and Hydraulic Engineering* vol. 2, no. 1, pp. 47–61, 1984.
- [20] N. Kouwen and T.E. Unny, "Flexible roughness in open channels," *Journal of the Hydraulics Division*, vol. 99, no. 5, pp. 713–728, 1973.
- [21] W. X. Huai, J. Zhang, W. J. Wang and G. G. Katul, "Turbulence structure in open channel flow with partially covered artificial emergent vegetation," *Journal of Hydrology*, vol. 573, pp. 180-193, 2019.
- [22] W. L. Cowan, "Estimating hydraulic roughness coefficients," *Agricultural Engineering*, vol. 37, no. 7, pp. 473–475, 1956.
- [23] [23] G. Eryılmaz Türkkkan, "Pürüzlülük katsayısının açık kanal akımına etkisinin incelenmesi", *Düzce Üniversitesi Bilim ve Teknoloji Dergisi*, vol. 9, no. 3, pp. 61–68, 2021.
- [24] M. Sunkar and S. Tonbul, "Batman'da 31 Ekim-1 Kasım 2006 tarihinde yaşanan taşkın nedenleri", in *II. Ulusal Taşkın Sempozyumu Tebliğler Kitabı*, Afyonkarahisar, Türkiye, 2010, pp. 349-361.
- [25] D. Öztürk, İ. Yılmaz and U. Kırbaş, "Çorum ili taşkın tehlikesinin analitik hiyerarşi yöntemi kullanılarak incelenmesi", in *TMMOB Harita ve Kadastro Mühendisleri Odası 16. Türkiye Harita Bilimsel ve Teknik Kurultayı*, Ankara, Türkiye, 2017, pp. 1-5.
- [26] E. E. Çanta, S. Temuçin Kılıçer and H. Akıncı, "FLO-2D ve HEC-RAS yazılımları ile Ardanuç (Artvin) ilçesindeki Pona Deresi ve Örtülü Deresi'nin taşkın yayılım haritalarının karşılaştırmalı üretilmesi," *Türk Uzaktan Algılama ve CBS Dergisi*, vol. 3, no. 1, pp. 50–64, 2022.